frontiers | Frontiers in Marine Science

ORIGINAL RESEARCH
published: 05 July 2022
doi: 10.3389/fmars.2022.920082

Anti-Inflammatory Effect of Acetone Extracts from Microalgae *Chlorella* sp. WZ13 on RAW264.7 Cells and TPA-induced Ear Edema in Mice

Longhe Yang[1], *Fan Hu*[1], *Yajun Yan*[1], *Siyu Yu*[1,2], *Tingting Chen*[1] *and Zhaokai Wang*[1]*

[1] *Technical Innovation Center for Utilization of Marine Biological Resources, Third Institute of Oceanography, Ministry of Natural Resources, Xiamen, China,* [2] *School of Traditional Chinese Materia Medica, Shenyang Pharmaceutical University, Shenyang, China*

Microalgae extracts have a wide range of uses in the field of healthcare and nutrition. However, the use of microalgae extracts in anti-inflammatory properties and their mechanism of action have not yet been fully studied. Here, we show that extracts from *Chlorella* sp. WZ13 (CSE-WZ13) dose-dependently reduced nitrite production, inhibited the expression of inducible nitric oxide synthase (iNOS) protein, and decreased the production of the gene and inflammatory cytokines tumor necrosis factor-α (TNF-α) and interleukin-6 (IL-6), in lipopolysaccharide (LPS)-stimulated RAW264.7 cells. Using high-content imaging analysis, it was found that CSE-WZ13 inhibited the translocation of nuclear factor kappa B (NF-κB) from the cytoplasm to the nucleus. CSE-WZ13 also exerted anti-inflammatory effects in an ear edema mouse model induced by 12-O-tetradecanoylphorbol-13-acetate (TPA). CSE-WZ13 inhibited edema by 36.17% and 25.66% at a dose of 0.3 and 0.1 mg/ear, respectively. Histological analysis showed that topical application of CSE-WZ13 decreased TPA-induced inflammatory cell infiltration. Our results indicate that CSE-WZ13 may be a useful candidate for the purpose of decreasing inflammation.

Keywords: microalgae, *Chlorella* sp., CSE-WZ13, RAW264.7, anti-inflammatory, edema, food

OPEN ACCESS

Edited by:
Ahmed M. Sayed, AlMaaqal University, Iraq

Reviewed by:
Abeer Elmaidomy, Beni-Suef University, Egypt
Yasmeen Ahmed, Nahda University, Egypt

***Correspondence:**
Zhaokai Wang
wang@tio.org.cn

Specialty section:
This article was submitted to Marine Biotechnology and Bioproducts, a section of the journal Frontiers in Marine Science

Received: *14 April 2022*
Accepted: *30 May 2022*
Published: *05 July 2022*

Citation:
Yang L, Hu F, Yan Y, Yu S, Chen T and Wang Z (2022) Anti-Inflammatory Effect of Acetone Extracts from Microalgae Chlorella sp. WZ13 on RAW264.7 Cells and TPA-induced Ear Edema in Mice. Front. Mar. Sci. 9:920082. doi: 10.3389/fmars.2022.920082

INTRODUCTION

Marine microalgae are rich sources of structurally diverse bioactive compounds due to their physiological ability to adapt to a wide range of marine environmental conditions, some of which are harsh (Carroll et al., 2021). It is estimated that the bioactive compounds found in algae species are 10 times more diverse than that found in taxonomic groups of land plants (Richmond and Hu, 2013). Microalgae produce many biologically active components, such as polyphenols, sulfated polysaccharides, terpenes, fatty acids, phycobilins, carotenoids, vitamins, and several other bioactive substances, which can be utilized as food additives to balance or increase nutrition (Vieira et al., 2020; Balasubramaniam et al., 2021; Ghosh et al., 2022). There are huge development prospects and market demands for microalgae because they or their components can be used to produce nutritious food for the elderly, formula food for unique medical purposes, unique dietary food, health food, and functional food (Vieira et al., 2020). Microalgae bio-products can also be used as topical agents for skin care to enhance the action of dermo-cosmetics and as attractive sources of materials for use in cosmeceutical industries (Berthon et al., 2017; Balasubramaniam et al., 2021; Obaid et al., 2021). A

number of microalgae extract-based skin products have already been marketed. Anti-aging moisturizers containing microalgae oil extracted from *Chlorella vulgaris* have been marketed as anti-wrinkle agents that nourish the skin because of all the vitamins, antioxidants, peptides, phytosterols, and essential fatty acids that are contributed by the algae (Thiyagarasaiyar et al., 2020).

Most reports have indicated that *Chlorella sorokiniana* is freshwater incubated and the extracts are rich in polyunsaturated fatty acids (PUFAs). It has been reported that the ethanol extract of *Chlorella sorokiniana* has the ability to inhibit cholinesterases, modulate the disaggregation of β-amyloid fibrils in cell models of Alzheimer's disease, and the main component of extract of this freshwater incubated microalgae are phenols, steroids, fatty acids, and terpenes as analyzed by GC-MS (Olasehinde et al., 2019). Importantly, *Chlorella sorokiniana* (UTEX 2805) lipid extracts, which contain unsaturated fatty acids and fatty acid methyl esters, improved short-term memory in rats (Morgese et al., 2016). The extracts also modulated cytokines secretion in sheep peripheral blood mononuclear cells (Ciliberti et al., 2019). G. Sibi also showed that lipid extracts from *Chlorella sorokiniana* inhibited lipase activity when exposed on antiacne treatment (Sibi, 2015). From a bioassay-guided study, Chou et al. identified a PPARγ-active fraction obtained from *Chlorella sorokiniana* W87 -10 extracts. This fraction showed typical signals of fatty acids as analyzed by ^{1}H- and ^{13}C-NMR spectra (Chou et al., 2008). Most recently, Lin et al. reported that *Chlorella sorokiniana* (W87) extract prevented cisplatin-induced myelotoxicity *in vitro* and *in vivo*, however, the main components were unrevealed (Lin et al., 2020). Yun and colleagues also reported that *Chlorella sorokiniana* KNUA114, which was collected from Ulleung Island South Korea, was rich in fatty acids and might potentially be used as biological resources (Yun et al., 2020). Other components from *Chlorella sorokiniana* extracts are also reported. For instance, polysaccharide exerts immunomodulatory effects in dendritic cells through NF-κB and PI3K/MAPK Pathways (Chou et al., 2012).

Although microalgae have a wide range of applications in functional health foods, drugs, potential manufacturing renewable algae biofuels and industrial chemicals (Camacho et al., 2019; M et al., 2019; Vieira et al., 2020; Jaiswal et al., 2021). However, the different species and different growth regions have great influence on their main material components and biological activities, due to the complex classification of microalgae, (Khan et al., 2018). The aim of the present study was to evaluate an acetone extract (CSE-WZ13), obtained from a seawater incubated strain of *Chlorella* sp. on the anti-inflammatory activity both in LPS induced RAW264.7 cells and TPA-induced ear edema in mice.

RESULTS

Identification of *Chlorella* sp. WZ13

The phenotypic characteristics of the WZ13 strain of microalgae are shown in **Figure 1A**. Small spherical unicellular microalgae with a single chloroplast with a pyrenoid were visible, which was consistent with a previously published description of genus Chlorella (Krienitz et al., 2015). The 18S rRNA gene sequence analysis indicated that the *Chlorella* sp. WZ13 strain belonged to the genus Chlorella and showed 99.89% sequence similarity to *Chlorella* sp. IFRPD and *Chlorella sorokiniana* UTEX2714, followed by *Chlorella sorokiniana* SAG 211-8k (99.83%), and *Chlorella sorokiniana* UTEX 2805 (99.83%). Thus, the *Chlorella* sp. WZ13 strain most likely belongs in the same family as *Chlorella sorokiniana*.

Extract and Compositional Analysis of *Chlorella* sp. WZ13

Chemical extraction and pre-fractionation of freeze-dried *Chlorella* sp. WZ13 were performed as the method reported by Lauritano et al. (Lauritano et al., 2016), and a flowchart of the extraction steps are shown in **Figure 1B**. We then analyzed the fatty acid composition of this extract by GC. Fatty acids in CSE-WZ13 (**Figure 2B**) are determined based on 37 component fatty acid methyl ester (FAME) standards mix (C4-C24) purchased from Sigma (Cat. No. 18919-1AMP) (**Figure 2A**). As shown in **Table 1**, the extract mainly contained medium long-chain saturated and unsaturated fatty acids. The total saturated fatty acid (SFA) content was 12.6%, which was dominated by palmitic acid (16:0). The total monounsaturated fatty acid (MUFA) content was 28.5%, of which oleic acid (18:1 c9) was the most abundant, at 17.7%. Palmitoleic acid (16:1 c9) was another MUFA present at a high level, at 5.5%. In this extract, the proportion of PUFAs was significantly higher than that of SFA and MUFA, accounting for 36% of the total fatty acid content. Of note, this extract contained 20.9% 9,12-octadecadienoic acid (18:2, t9, t12) and 15.1% linolenic acid (18:3, c6, c9, c12).

Detection of free fatty acids by GC requires methylation. Therefore, we don't know whether the detailed original composition of the fatty acids in CSE-WZ13 is the free fatty acids or fatty acid methyl esters (FAMEs). We then analyzed the crude extraction components of CSE-WZ13 using nuclear magnetic resonance (NMR). The ^{1}H NMR spectrum of CSE-WZ13 showed that most protons represented aliphatic protons in the region between 0.5 and 2.5 ppm. These protons along with the peaks at 5.3 ppm indicated the presence of olefinic protons on unsaturated fatty acids (**Figure 3**). Since the integrals of methoxy protons and other protons are not proportional, we judged that the crude extracts were still dominated by free fatty acids, while including some FAMEs, with small proportion

CSE-WZ13 Reduced Nitrite Production and iNOS Expression in LPS-Induced RAW264.7 Cells

We used LPS-induced RAW264.7 cells to evaluate the biological activity of the extract. We first determined the level of cytotoxicity to RAW264.7 cells by CSE-WZ13. As shown in **Figure 4A**, the extract was not cytotoxic to RAW264.7 cells up to 30 μg/ml. To assess the anti-inflammatory effects of CSE-WZ13, RAW264.7 cells were treated with various concentrations of the extract ranging from 3 to 30 μg/ml, with dexamethasone (Dex, 5 μg/ml) as a positive control, and the effects of CSE-WZ13 on the

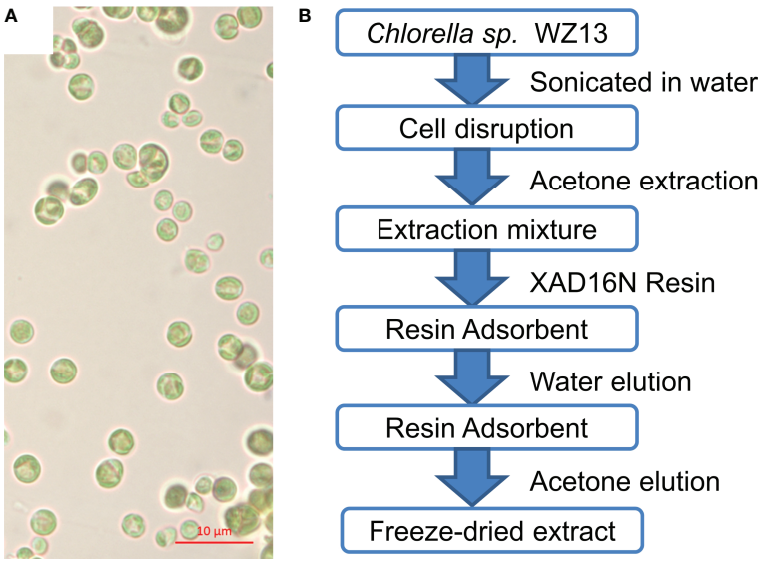

FIGURE 1 | Morphology of microalgae *Chlorella* sp. WZ13 and illustration of the process used to obtain the freeze-dried algal extract (CSE-WZ13). **(A)** Microscopic observation of *Chlorella* sp. WZ13 (under mineral oil 100× magnification; scale bar = 10 μm). **(B)** Extraction steps performed to obtain the freeze-dried extract CSE-WZ13 from *Chlorella* sp. WZ13.

production of nitrite in LPS-stimulated RAW264.7 cells were determined by Griess reagent. It was shown that LPS (1 μg/ml) treatment significantly increased the levels of nitrite in the culture medium of RAW264.7 cells. Treatment with CSE-WZ13 (3-30 μg/ml) dose-dependently decreased the levels of nitrite by 71.3%, 46.4%, and 24.8% compared with the group treated only with LPS (**Figure 4B**). More importantly, the effect of high concentration of CSE-WZ13 (30 μg/ml) on LPS induced nitrite induction was comparable to that of positive control dexamethasone treatment (71.3% vs. 70.0%).

It is known that inducible nitric oxide synthase (iNOS) regulates inflammatory reactions and catalyzes the synthesis of nitrite. Therefore, we further tested the alteration of iNOS protein expression following CSE-WZ13 and dexamethasone treatment in LPS-induced RAW264.7 cells. As shown in **Figure 4C**, CSE-WZ13 and dexamethasone treatment inhibited LPS-induced iNOS protein expression in a dose concentration-dependent manner. These results provide evidence that CSE-WZ13 inhibited the production of nitrite by suppressing iNOS protein expression in LPS-stimulated RAW264.7 cells.

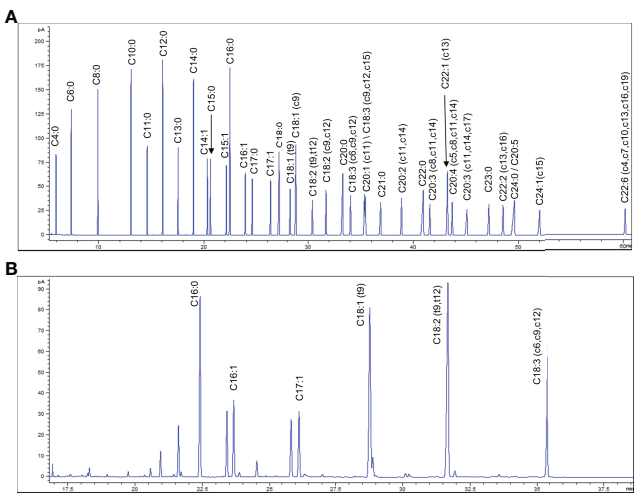

FIGURE 2 | GC analysis of FAMEs standards Mix and CSE-WZ13. **(A)** Chromatography of 37 component FAMEs standards Mix (C4-C24). **(B)** Chromatography of FAMEs in CSE-WZ13.

CSE-WZ13 Decreased the Amounts of Pro-Inflammatory Cytokines and mRNA Expression in LPS-Induced RAW264.7 Cells

To further assess the effects of CSE-WZ13 on the expression of pro-inflammatory cytokines in LPS-treated RAW264.7 cells, we first evaluated the effects of CSE-WZ13 on the expression of TNF-α and IL-6 mRNA expression in LPS-induced RAW264.7 cells. It was shown that LPS treatment significantly increased the

TABLE 1 | Fatty acid composition of CSE-WZ13[1].

No.	Lipid name		Relative%
1	Palmitic acid	C16:0	12.6
2	Palmitoleic acid	C16:1	5.5
3	10-Heptadecenoic acid	C17:1	5.3
4	Oleic acid	C18:1	17.7
5	linoleic acid	C18:2	20.9
6	linolenic acid	C18:3	15.1

[1]*The data are expressed as a % of the total fatty acid methyl esters (FAME).*

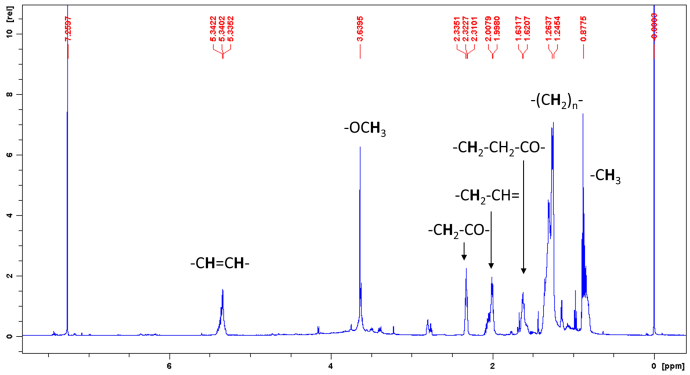

FIGURE 3 | ^{1}H NMR spectrum and profiling of CSE-WZ13.

TNF-α and IL-6 mRNA expression of RAW264.7 cells. However, treatment with CSE-WZ13 dose-dependently repressed the mRNA expression of TNF-α and IL-6 (**Figures 5A, B**). We further quantitated the cytokines of TNF-α and IL-6 in the culture medium by enzyme-linked immune sorbent assay (ELISA) assays. As show in **Figures 5C, D**, CSE-WZ13 significantly reduced TNF-α and IL-6 factors which increased by LPS treatment in a dose dependent manner. Although dexamethasone treatment at 5 μg/ml showed significant anti-cytokines effects among these administration groups, which was comparable to CSE-WZ13 at 30 μg/ml, and even had a more pronounced inhibitory effect on TNF-α production. These results indicated that CSE-WZ13 suppressed the expression of these pro-inflammatory mediators in LPS-treated RAW264.7 cells.

CSE-WZ13 Inhibited Cytosolic to Nuclear Translocation of NF-κB

Given the NF-κB signaling that occurs during the regulation of cytokine production, we tested the hypothesis that CSE-WZ13 modulates NF-κB in the cytosolic to nuclear translocation in LPS-induced RAW264.7 cells. We used a high-content screening system to image the NF-κB p65 subunit in RAW264.7 cells. As shown in **Figures 6A, B**, NF-κB is located in the cytosol in vehicle- and CSE-WZ13-treated cells. However, LPS treatment induced NF-κB translocation from the cytosol to the nucleus in most of the cells. CSE-WZ13 treatment dose-dependently inhibited NF-κB translocation from the cytoplasm to the nucleus. These results suggest that CSE-WZ13 inhibited NF-κB activation in RAW264.7 cells.

CSE-WZ13 Inhibited TPA-Induced Ear Edema in Mice

Based on the anti-inflammatory action of CSE-WZ13 in LPS-stimulated RAW264.7 cells, we then examined the effect of CSE-WZ13 *in vivo*. We used TPA to establish mouse ear swelling and then evaluated skin inflammation by ear weight and histology analysis. Dexamethasone (0.1 mg/ear) treatment as positive control. After topical treatment of TPA, mouse ear tissue

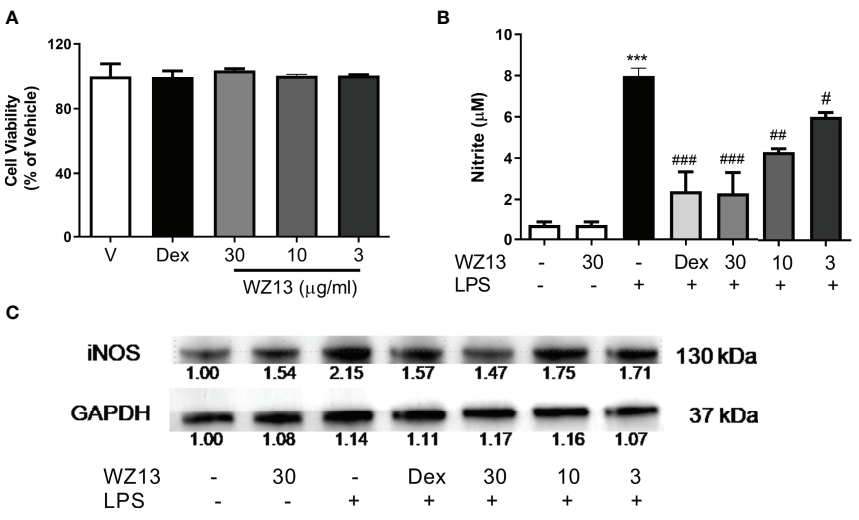

FIGURE 4 | Effects of CSE-WZ13 (WZ13) and dexamethasone (Dex, 5 μg/ml) on **(A)** cell viability, **(B)** LPS-induced nitrite production, and **(C)** iNOS expression in RAW264.7 macrophages. iNOS expression was calculated based on the vehicle (-)-treated control. Data are presented as mean ± SEM (n=3) in **(A, B)** ***P < 0.001 compared with vehicle-treated group, #P < 0.05, ##P < 0.01, ###P < 0.001 compared with LPS-treated group.

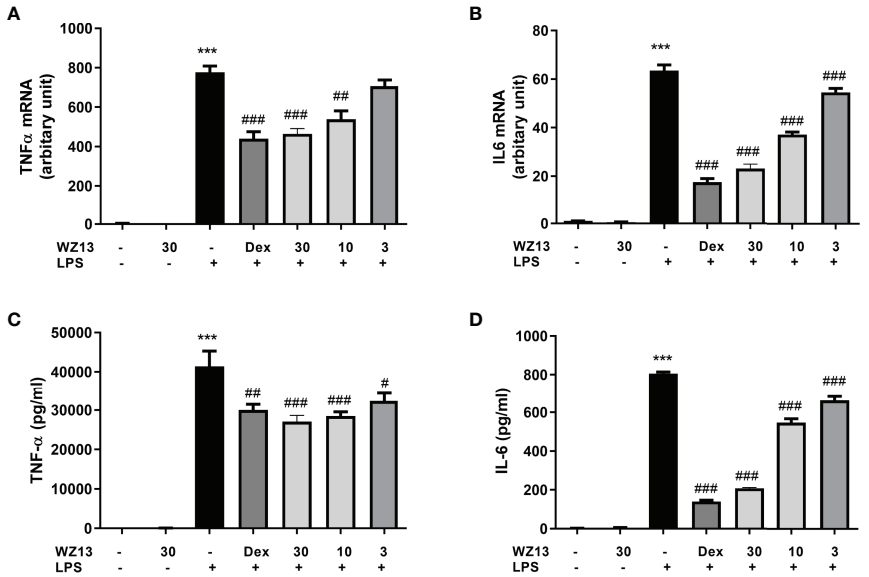

FIGURE 5 | Anti-inflammatory effects of CSE-WZ13 (WZ13) and dexamethasone (Dex, 5 μg/ml) on RAW264.7 cells. The mRNA expression of TNF-α **(A)** and IL-6 **(B)** in LPS-treated RAW264.7 cells. Pro-inflammatory mediators TNF-α **(C)** and IL-6 **(D)** in the supernatant of LPS-treated RAW264.7 cells. Data are presented as mean ± SEM (n=3) ***P < 0.001 compared with the vehicle-treated group, #P < 0.05, ##P < 0.01, ###P < 0.001 compared with the LPS-treated group.

edema was intense as determined by the increase of ear weight, when compared to vehicle-treated control ear (**Figure 7F**). It was observed that topical treatment of 0.1 mg/ear dexamethasone (Dex), 0.3 and 0.1 mg/ear CSE-WZ13 significantly reduced auricle edema by 60.99%, 40.85%, and 28.82%, respectively (**Figure 7E**). Histological analysis of the TPA treated ears uncovered a significant increase in dermis thickness which was accompanied by a large number of inflammatory cells infiltration. Connective tissue loosening and fibers from extracellular matrix disorganization were also observed (**Figure 7B**) when compared to vehicle-treated ear (**Figure 7A**). The ears topically treated with 0.1 mg/ear Dex positive control (**Figure 7C**), 0.3 and 0.1 mg/ear CSE-WZ13 (**Figures 7D, E**) showed lower dermis thickness and a significant reduction in inflammatory cells infiltration when compared to the TPA treated ear (**Figure 7B**).

DISCUSSION

The active constituents of marine microalgae include fatty acids, carotenoids, polysaccharides, polyphenols, and proteins. In the current study, a resin that mainly adsorbs non-polar substances was used to fractionate the acetone extract from marine microalga *Chlorella* sp. WZ13. Consistent with previous studies (Chou et al., 2008; Iglesias et al., 2019), the extracts were mainly composed of fatty acids, according to the ^{1}H-NMR spectrum (**Figure 3**). However, the types of free fatty acids produced by different marine microalgae were quite different, which also deeply affected the biological activity of the marine microalgae extracts. As reported by Chou et al. (Chou et al., 2008), the main constituent of fatty acid from CE 3-3 was saturated fatty acid C16:0, which relative proportion was about 43.6%. In this study, we found that the main contents of fatty acids from CSE-WZ13 were unsaturated fatty acid as linoleic acid (C18:2, 20.9%), oleic acid (C18:1, 17.7%), and linolenic acid (C18:3, 15.1%). The proportion of saturated fatty acids was very small, and C16:0 only accounted for about 12.6% (**Table 1**). However, we can't rule out a small proportion of the pharmacological effects of FAMEs, since it can be indentified in ^{1}H NMR. In future research, more separation and analysis methods should be applied to determine the detailed derivatives of the original methylesterification products in CSE-WZ13.

PUFAs are very important for maintaining human health, preventing heart disease, and inhibiting tumor cell growth through anti-oxidation and anti-inflammation (Remize et al., 2021). PUFAs derived from microalgae are considered to be excellent substitutes for deep-sea fish oil, which can satisfactorily relieve inflammation. However, we did not detect the presence of a large amount of docosahexaenoic acid (DHA) or eicosapentaenoic acid (EPA) in CSE-WZ13 (**Table 1**). Therefore, the abundant linoleic acid and linolenic acid in the acetone extract may contribute to the observed biological activity. The beneficial physiological effects of linoleic acid and linolenic acid on the inflammatory response have been widely recognized (Wen et al., 2019; Marangoni et al., 2020). They can regulate the production of inflammatory cytokines, including IL-6, TNF-α, and IFN-γ, which may be related to the activation of nuclear transcription factor PPAR-γ (Bassaganya-Riera et al., 2004).

Inflammation is a complicated response to infection, injury, and stress. Macrophages are the most widely distributed and dominant immune cells in the body and play a crucial role in innate and adaptive immune responses, including inflammation. Normally, macrophages have a beneficial protective role in acute inflammation. However, chronic inflammatory responses

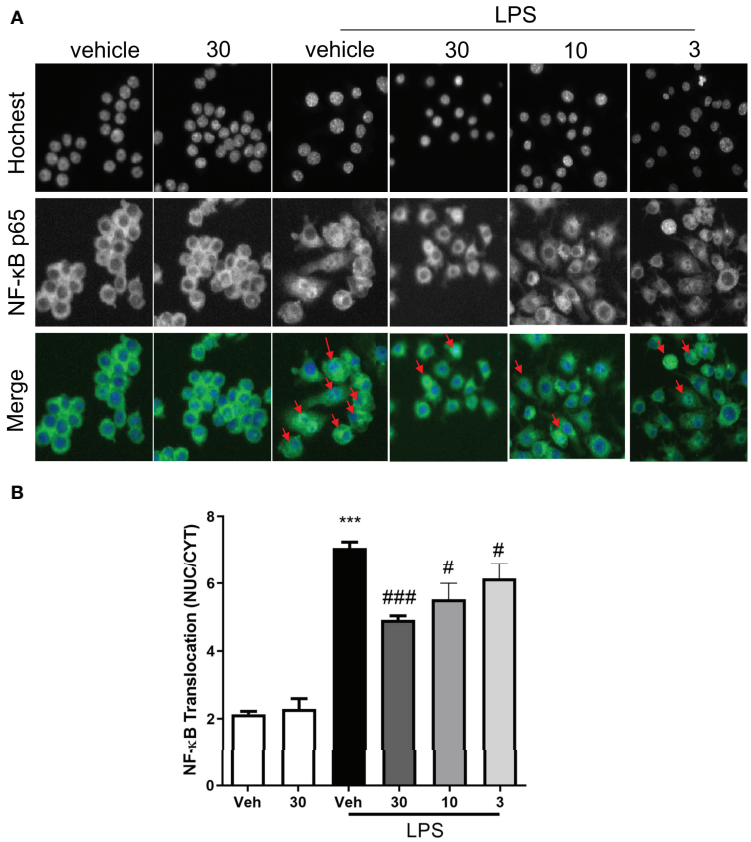

FIGURE 6 | CSE-WZ13 inhibited the translocation of NF-κB from the cytoplasm to the nucleus in LPS treated RAW264.7 cells. **(A)** Representative pictures from the DAPI (Hochest 33342) and FITC (NF-κB p65) channel, the red arrows show the entry of NF-κB p65 into the nucleus. **(B)** The average pixel intensity was measured in the nucleus and cytoplasm of each cell, and a translocation value was calculated by NUC/CYT. Data are presented as mean ± SEM (n=8) ***P < 0.001 compared with the vehicle-treated group, #P < 0.05, ###P < 0.001 compared with the LPS-treated vehicle group.

induced by endotoxins and inflammatory mediators in macrophages lead to overproduction of inflammatory mediators such as cytokines and chemokines. These results were involved in the development of chronic inflammatory diseases, including allergies, chronic pain, atherosclerosis, rheumatoid arthritis, neurological disorders, diabetes, and lung diseases (Meizlish et al., 2021). The RAW264.7 cell line was established from Abelson murine leukemia virus-induced tumors and is easily propagated and suitable for *in vitro* culture. LPS is a component of Gram-negative bacteria and induces the secretion of pro-inflammatory mediators by binding toll-like receptor 4 and activating a number of intracellular signaling pathways. Therefore, LPS-stimulated macrophage models have been widely used to study the anti-inflammatory effects of candidate substances (He and Ma, 2020; Jin et al., 2020). In the present study, LPS-induced RAW264.7 macrophages were used to evaluate the anti-inflammatory effects of CSE-WZ13. LPS stimulates macrophages to produce large amounts of iNOS, which induces nitric oxide (NO) production (Orecchioni et al., 2019). Nitrites are extensively involved in the regulation of physiological functions and the development of pathological processes. iNOS is the rate-limiting enzyme for NO synthesis. Over-expression of NO and iNOS is significantly correlated with the progression of various inflammatory diseases. CSE-WZ13 pretreatment inhibited LPS-induced NO production by RAW264.7 cells (**Figure 4B**) as well as iNOS (**Figure 4C**) expression. These results suggested that CSE-WZ13 exerted an anti-inflammatory effect on the LPS-induced inflammatory response. In the inflammatory response, membrane recognition receptors on the surface of macrophages are stimulated by LPS to activate the inflammatory pathway and produce pro-inflammatory cytokines (Viola et al., 2019). In many chronic inflammatory diseases, such as rheumatoid arthritis (Chen et al., 2019), osteoarthritis (Chow and Chin, 2020), and psoriasis (de Alcantara et al., 2021), inflammatory factors such as IL-6 and TNF-α are significantly elevated. Blockade of IL-6 and TNF-α by antibodies has been shown to be effective in the treatment of these diseases (Senolt, 2019; Pandolfi et al., 2020). In the current study, we examined whether CSE-WZ13 inhibits the LPS-induced production of cytokines. The results showed that CSE-WZ13 pretreatment dose-dependently inhibited LPS-induced TNF-α and IL-6 production in RAW264.7 cells (**Figure 5**).

Oxidative stress is an important factor in inflammatory lesions that appear in several diseases, and the NF-κB signaling pathway is one of the major pathways in the inflammatory signal transduction

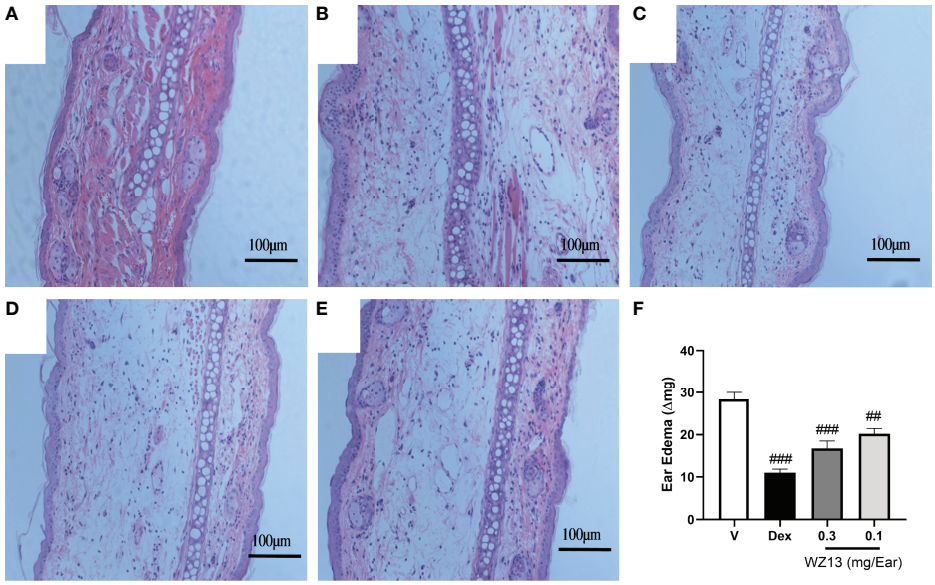

FIGURE 7 | CSE-WZ13 inhibited ear edema in mice treated with TPA. Representative images of histological transversal cuts of mouse ears and analysis of alterations induced by **(A)** vehicle, **(B)** TPA, **(C)** 0.1 mg/ear dexamethasone (Dex), **(D)** 0.3 mg/ear CSE-WZ13, and **(E)** 0.1 mg/ear CSE-WZ13; **(F)** ear edema as measured by ear weight. Data are presented as mean ± SEM (n=8) $^{###}P < 0.001$, $^{##}P < 0.01$ compared with vehicle-treated group.

pathway (Kunnumakkara et al., 2020). NF-κB includes five components, p65 (RelA), p50/p105, p52/p100, c-Rel, and Rel-B, which form various heterodimers or homodimers. Under normal conditions, NF-κB exists as an inactive heterotrimer, including p50, p65 (Rel A), and IκB, in the cytosol. Once stimulated by LPS, cytokines, or stress, IκB phosphorylates dissociate from NF-κB. Thus, NF-κB translocates into the nucleus, attaches to specific DNA-binding elements, and induces the expression of inflammatory genes such as iNOS and other pro-inflammatory cytokines such as IL-6 and TNF-α. Therefore, inhibition of the NF-κB signaling pathway is one of the main targets for the treatment of inflammatory diseases (Tasneem et al., 2019). Here, a high-content image was obtained to confirm that pretreatment with CSE-WZ13 in RAW264.7 cells significantly inhibited LPS-induced translocation of NF-κB p65 subunits to the nucleus (**Figure 6**). Thus, the production of IκB reduced the nuclear transcription of NF-κB and downregulated the expression of pro-inflammatory factors and the inflammatory response.

TPA is a common inflammatory mediator that is involved with vascular permeability alteration, macrophage activation, inflammatory cell aggregation, and pro-inflammatory mediator secretion (Yang et al., 2015). In this experiment, we used quality difference analysis and HE staining and observed that the degree of swelling, induced by TPA, of inflamed mouse ears was significantly higher than those of vehicle ears, which indicated a successful modeling. A single topical treatment of CSE-WZ13 at concentrations of 0.3 mg/ear significantly reduced the ear swelling induced by TPA (**Figure 7**). This inhibitory effect was accompanied by a reduction in inflammatory cells infiltration as revealed by histological analysis. The doses we used in this paper (0.3mg and 0.1mg/ear) showed moderate activity compared to the reference drug dexamethasone (0.1 mg/ear) in this paper and reported by other research groups (Ascari et al., 2019; Rocha et al., 2020).

Marine microalgae extracts play an important role in host immune regulation and inflammation-related diseases, and therefore, such extracts have great application values and research prospects in the medical field (Riccio and Lauritano, 2019). However, the main chemical composition and regulation mechanisms of microalgae extracts are still unclear. Our experiments provide information that is beneficial for many research fields.

In conclusion, we have described the main chemical composition of CSE-WZ13 were medium long-chain saturated and unsaturated fatty acids which were preliminarily clarified through nuclear magnetic resonance (NMR) and gas chromatography (GC) analysis. The CSE-WZ13 biological activity was first examined by conducting *in vitro* experiments with LPS stimulated RAW264.7 cells and showed that it inhibited the expression of inducible nitric oxide synthase (iNOS) protein, and decreased the production of the inflammatory cytokine tumor necrosis factor-α (TNF-α) and interleukin-6 (IL-6). Moreover. CSE-WZ13 inhibited the translocation of NF-κB from the cytoplasm to the nucleus in LPS stimulated RAW264.7 cells. Finally, CSE-WZ13 also inhibited era edema in TPA induced mouse era inflammatory model. Our results indicated that CSE-WZ13 may be a candidate additive for anti-inflammatory foods. In-depth studies on anti-inflammatory mechanisms, optimal dosage, safety, and metabolic transformation will provide additional valuable data and are worthy of being carried out.

MATERIALS AND METHODS

Microalgae Cultivation

Chlorella sp. WZ13 was isolated from Xinglin Bay, Xiamen, China, by the enrichment technique on the f/2 culture medium and was deposited in the Marine Medicinal Organism Germplasm Resources Bank of Third Institute of Oceanography (MMOGRB0046). Whole-genome shotgun sequencing was performed using a Nanopore platform at the Beijing Genomic Institute (BGI, Shenzhen, China). Wtdbg2 was used for fast and accurate long-read genome assembly (https://github.com/ruanjue/wtdbg2). The predicted 18s RNA sequences were extracted from the genome sequence by Rfam 12.0+ (http://rfam.xfam.org/), and then blasted against the nt database. To grow it, we used f/2 culture medium, which contained 10 g/L of glucose, 2 g/L of tryptone, 1 g/L of yeast extract, and 1 g/L of bacteriological peptone supplement, and then adjusted the medium to 15% salinity by mixing seawater and distilled water. The pH of the prepared nutrient medium was adjusted to 6, and then the medium was sterilized at 115°C for 30 min. Under aseptic conditions, pure algae were selected from a culture plate, inoculated into 100-mL medium, and cultured at 25°C and 120 rpm in a dark environment for 3–5 days.

When microalgae growth was evident, the culture was used as a seed liquid that was inoculated into 3000 mL of medium and grown at 25°C with 200 rpm magnetic stirring for 8–10 days. To collect the wet algae, the culture medium was centrifuged at 8000 rpm for 10 min, and the pellet was then weighed. The wet algae were freeze-dried at −80°C for 3 days, and the algae powder was maintained at −80°C until extraction.

Preparation of Extract

The extraction of CSE-WZ13 and pre-fractionation were performed as previously reported, with minor changes (Lauritano et al., 2016). Briefly, 1 g of freeze-dried microalgae was added to 5 ml of distilled water and sonicated for 3 min at maximum intensity on ice. Next, 5 mL of acetone was added, and the liquid was incubated for 50 min at room temperature on an orbital shaker. The acetone was then evaporated under a nitrogen stream, and 1 g of Amberlite® XAD16N (Sigma-Aldrich, Shanghai, China) polymeric adsorbent resin was added to bind the non-polar solute from the water. After 50 min of mixing at room temperature, the sample was centrifuged at 5000 x g for 15 min. After elution with 10 ml of water, the resin pellet was washed with 5 ml of acetone. The acetone elution containing the microalgae extract was collected, freeze-dried after nitrogen stream evaporate acetone, and stored at −20°C until bioactivity screening. The yield of CSE-WZ13 was 67.1 mg (*voucher number: CACC0046)*. The extract was diluted in dimethyl sulfoxide (DMSO) for use in cell culture assays.

NMR (Nuclear Magnetic Resonance) Analyses of CSE-WZ13

The extraction of CSE-WZ13 was dissolved in 500 μL $CDCl_3$ and transferred into a 5 mm NMR tube for identification of compounds. NMR experiments were performed using 1H NMR (BRUKER AVANCE III 600 MHz HD NMR spectrometer) equipped with BBO probe at 300 K. A ^{1}H-NMR spectrum was recorded with chemical shift in parts per million (ppm) from tetramethylsilane (TMS) as an internal standard.

Hydrolysis and Esterification of Lipids

The extracted CSE-WZ13 was mixed with 2 mol/L KOH methanol solution at 80 °C for hydrolysis with 70 Hz ultrasonic for 2 h. After cooling, 3 mL 50% boron trifluoride (BF3)-methanol solution was added in and ultrasonic hydrolyzed at 70 Hz for 2 h at 60°C. The mixture was treated with 3 mL hexane to extract fatty acid methyl esters. The lipid layer was separated from methanol by centrifugation at 5000 rpm for 5 min. The organic phase was then collected and dried under nitrogen flow. Dried fatty acid methyl esters were re-dissolved in 1 mL hexane and loaded into a 1.5 mL vial for further gas chromatography (GC) analyses.

Gas Chromatography (GC) Analyses

The fatty acid methyl esters were identified using GC (Agilent) equipped with a capillary column (Agilent CP SIL 88, 0.25 μm x 0.25 μm x 100 m). Briefly, initial temperature was set at 100°C and held for 5 min. Temperature increased from 100 to 180°C at a rate of 8°C min-1 and held for 9 min on reaching 180°C. Temperature was further increased from 200 to 230°C at a rate of 1°C min-1 and held for 15 min on reaching 230°C. He was chosen as the carrier gas with a flow rate of 40 mL/min. The detector gas flow rate was set as 400 mL/min for air and 40 mL/min for H2. Data were compared with the standard FAME mix (C4-C24) purchased from Sigma (Cat. No. 18919-1AMP).

RAW264.7 Cell Culture and Treatment

RAW264.7 mouse macrophage cells were cultured in Dulbecco's modified Eagle's medium (DMEM) with 10% fetal bovine serum (FBS) and antibiotics (100 units/mL of penicillin and 100 μg/mL of streptomycin) and maintained in a humidified 5% CO_2 incubator at 37°C. For the experiment, RAW264.7 cells were seeded overnight into 24-well plates, with 1×10^5 cells per well. The next day, the cells underwent lipopolysaccharide (LPS) treatment (1 μg/ml) and were then incubated with fresh culture medium containing the indicated concentration of the compounds for 30 min. Cells were treated with vehicle (DMSO, 0.1%) as the control.

Nitrite and Cytokines Quantification

The concentration of nitrite in the culture medium was determined by a Griess Reagent Kit (Thermo Fisher, Shanghai, China). Briefly, 75 μL of cell culture supernatants were reacted with 65 μL of distilled water and 10 μL of Griess reagent for 30 min at room temperature, and the absorbance of the diazonium compound was obtained at a wavelength of 560 nm.

Mouse TNF-α and IL-6 in Raw264.7 cells supernatant were measured by Valukine™ ELISA kit (R&D Systems, Cat no. VAL609 and VAL604, Shanghai, China) according to manufacturer protocols.

RNA Isolatation and Quantitative Real-Time PCR (qRT-PCR)

Total RNA was extracted from RAW264.7 cells using TRIzol reagent (Life technologies, Carlsbad, CA, USA) following the manufacturer's protocol. cDNA was synthesized from 1μg mRNA by ReverTra Ace®qPCR RT Master Mix (Toyobo, Shanghai, China) according to the manufacturer's protocol. Finally, qRT-PCR was quantified on a Roche LightCycler 96 system by using Platinum SYBR Green qPCR SuperMix-UDG with ROX (Invitrogen, Shanghai, China), and the relative mRNA expression of each gene were calculated using the $2^{-\Delta\Delta CT}$ method and normalized to GAPDH. The first-stranded cDNA was amplified using the following primers: TNF-α, 5'-GTAGCAAACCACCAAGTGGAGG-3'(forward) and 5'-CAGCCTTGTCCCTTGAAGAGAA-3' (reverse); IL-6, 5'-AATTAAGCCTCCGACTTGTGAAG-3'(forward) and 5'-CTTCCATCCAGTTGCCTTCTTG-3' (reverse); GAPDH, 5'ACCACGAGAAATATGACAACTCCC-3' (forward) and 5'-CCAAAGTTGTCATGGATGACC-3' (reverse).

NF-κB Nuclear Translocation Assay

The NF-κB nuclear translocation assay was conducted as previously reported (Niu et al., 2020). Briefly, RAW264.7 cells were seeded at 2×10^4 cells/well in 96-well plates in DMEM medium containing 10% FBS and antibiotics (100 units/mL of penicillin and 100 μg/mL of streptomycin) overnight at 37°C in a humidified 5% CO2 incubator. After LPS challenge (1 μg/ml) for another 60 min, the cells were treated with CSE-WZ13 or vehicle (DMSO) for 30 min. Cells were then fixed with 4% paraformaldehyde for 15 min at room temperature (RT). Cells were washed once with phosphate-buffered saline (PBS) and incubated at RT for 5 min in 100 μl of 0.1% Triton X-100/PBS. Cells were stained with primary rabbit anti-NF-κB-p65 polyclonal antibody (Cell Signaling Technology, Shanghai, China) at a dilution ratio of 1:400 in PBS and then incubated for 60 min at RT. Cells were washed and stained with Alexa Fluor 488 conjugate goat anti-rabbit IgG (H+L) secondary antibody (Cell Signaling Technology, Shanghai, China) at a final concentration of 2 μg/mL in PBS containing 1 μg/mL Hoechst 33342 for 1 h in the dark.

Plates were washed and maintained in PBS and imaged with a Cellomics ArrayScan VTI High-Content Screening Reader (Thermo Fisher) using 4',6-diamidino-2-phenylindole (DAPI) and fluorescein isothiocyanate (FITC) channels at 10 × magnification. Four fields were captured for each well. Images were analyzed using HCS Studio: Cellomics Scan Version 6.6.0 software (Thermo Fisher).

12-O-Tetradecanoylphorbol-13-Acetate (TPA)-Induced Ear Edema in Mice

Ear edema in mice was induced by TPA according to a previously reported protocol (Yang et al., 2015). Briefly, male C57BL6/J (22–25 g) mice were obtained from Shanghai SLAC Laboratory Animal Co. Ltd. and housed with food and water ad libitum at a temperature of 22°C, 70% humidity, and 12-h light/dark cycles. All animal experiments were conducted in accordance with the Association for Research at the Third Institute of Oceanography, Statement for the Use of Animals in Pharmacological Research guidelines and were approved by the Experimental Animal Ethics Committee of the Third Institute of Oceanography, Ministry of Natural Resources under license number TIO-IACUC-04-2020-06-22.

TPA (0.03% in acetone, 20 μL) was applied to the external and internal ear, and the same volume of acetone was applied to the matched right ears as a control. CSE-WZ13 was dissolved in acetone at 1.5% and 0. 5% (w/v) and then applied 20 μL topically on both ears which equal to 0.3 and 0.1 mg/ear. Dexamethasone treatment (0.1 mg/ear) as positive control. After 30 min, the TPA solution was administered, and 3 h after inflammatory agent administration, the mice were euthanized by cervical dislocation. Circular sections 8 mm in diameter were taken from both the treated (t) and non-treated control ears (ctrl) using an Electric Animal Ear Punch (YLS-25A, Ji'nan, Shandong, China). Ear tissues were immediately weighed to assess edema and subsequently immersed in 4% paraformaldehyde solution for hematoxylin and eosin (H&E) assay. Ear edema was obtained as:

$$\triangle w = w(t) - w(ctrl).$$

Histological Analysis

After mouse ear tissues were fixed in 4% paraformaldehyde for 1 day, they were dehydrated in a series of ethanol solutions and then embedded in paraffin. Next, the tissues were cut into 5 μm thick sections by using a Leica SM2010 R sliding microtome (Shanghai, China) and were then stained with H&E after deparaffinization with xylene. Images were obtained with a light microscope (Nikon, Shanghai, China).

Data Analysis

All data are expressed as the mean ± SEM (standard error of the mean), and statistical significance was evaluated by using an analysis of variance (ANOVA), followed by Dunnett's test for multiple comparisons. Values were considered significant at $p \leq 0.05$.

DATA AVAILABILITY STATEMENT

The original contributions presented in the study are included in the article/supplementary material. Further inquiries can be directed to the corresponding author.

ETHICS STATEMENT

This study was conducted in accordance with the Association for Research at the Third Institute of Oceanography, Statement for the Use of Animals in Pharmacological Research guidelines, and was approved by the Experimental Animal Ethics Committee

of the Third Institute of Oceanography, Ministry of Natural Resources under license number TIO-IACUC-04-2020-06-22.

AUTHOR CONTRIBUTIONS

Conceptualization, ZW and LY; methodology, LY, FH, and YY; formal analysis, SY and TC; investigation, FH; resources, ZW; data analysis, LY and FH; writing—original draft preparation, LY and FH; writing—review and editing, ZW; supervision, ZW; funding acquisition, LY and ZW. All authors have read and agreed to the published version of the manuscript.

FUNDING

This research was funded by "Scientific Research Foundation of Third Institute of Oceanography, Ministry of Natural Resources, grant number 2019023, 2020010" and "the Fujian Provincial Natural Science Foundation, grant number 2020N0028".

ACKNOWLEDGMENTS

We thank Dr. Yan Qiu for helpful results discussion, we also thank LetPub (www.letpub.com) for its linguistic assistance during the preparation of this manuscript.

REFERENCES

Ascari, J., de Oliveira, M. S., Nunes, D. S., Granato, D., Scharf, D. R., Simionatto, E., et al. (2019). Chemical Composition, Antioxidant and Anti-Inflammatory Activities of the Essential Oils From Male and Female Specimens of Baccharis Punctulata (Asteraceae). *J. Ethnopharmacol.* 234, 1–7. doi: 10.1016/j.jep.2019.01.005

Balasubramaniam, V., Gunasegavan, R. D., Mustar, S., Lee, J. C. and Mohd Noh, M. F. (2021). Isolation of Industrial Important Bioactive Compounds From Microalgae. *Molecules* 26 (4), 934. doi: 10.3390/molecules26040943

Bassaganya-Riera, J., Reynolds, K., Martino-Catt, S., Cui, Y., Hennighausen, L., Gonzalez, F., et al. (2004). Activation of PPAR Gamma and Delta by Conjugated Linoleic Acid Mediates Protection From Experimental Inflammatory Bowel Disease. *Gastroenterology* 127 (3), 777–791. doi: 10.1053/j.gastro.2004.06.049

Berthon, J. Y., Nachat-Kappes, R., Bey, M., Cadoret, J. P., Renimel, I. and Filaire, E. (2017). Marine Algae as Attractive Source to Skin Care. *Free Radic. Res.* 51 (6), 555–567. doi: 10.1080/10715762.2017.1355550

Camacho, F., Macedo, A. and Malcata, F. (2019). Potential Industrial Applications and Commercialization of Microalgae in the Functional Food and Feed Industries: A Short Review. *Mar. Drugs* 17 (6), 312. doi: 10.3390/md17060312

Carroll, A. R., Copp, B. R., Davis, R. A., Keyzers, R. A. and Prinsep, M. R. (2021). Marine Natural Products. *Nat. Prod. Rep.* 38 (2), 362–413. doi: 10.1039/d0np00089b

Chen, Z., Bozec, A., Ramming, A. and Schett, G. (2019). Anti-Inflammatory and Immune-Regulatory Cytokines in Rheumatoid Arthritis. *Nat. Rev. Rheumatol.* 15 (1), 9–17. doi: 10.1038/s41584-018-0109-2

Chou, N. T., Cheng, C. F., Wu, H. C., Lai, C. P., Lin, L. T., Pan, I. H., et al. (2012). Chlorella Sorokiniana-Induced Activation and Maturation of Human Monocyte-Derived Dendritic Cells Through NF-kappaB and PI3K/MAPK Pathways. *Evid. Based. Complement. Alternat. Med.* 2012, 735396. doi: 10.1155/2012/735396

Chou, Y. C., Prakash, E., Huang, C. F., Lien, T. W., Chen, X., Su, I. J., et al. (2008). Bioassay-Guided Purification and Identification of PPARalpha/gamma Agonists From Chlorella Sorokiniana. *Phytother. Res.* 22 (5), 605–613. doi: 10.1002/ptr.2280

Chow, Y. Y. and Chin, K. Y. (2020). The Role of Inflammation in the Pathogenesis of Osteoarthritis. *Mediators Inflammation* 2020, 8293921. doi: 10.1155/2020/8293921

Ciliberti, M. G., Albenzio, M., Francavilla, M., Neglia, G., Esposito, L. and Caroprese, M. (2019). Extracts From Microalga Chlorella Sorokiniana Exert an Anti-Proliferative Effect and Modulate Cytokines in Sheep Peripheral Blood Mononuclear Cells. *Anim. (Basel).* 9 (2), 45. doi: 10.3390/ani9020045

de Alcantara, C. C., Reiche, E. M. V. and Simao, A. N. C. (2021). Cytokines in Psoriasis. *Adv. Clin. Chem.* 100, 171–204. doi: 10.1016/bs.acc.2020.04.004

Ghosh, S., Sarkar, T., Pati, S., Kari, Z. A., Edinur, H. A. and Chakraborty, R. (2022). Novel Bioactive Compounds From Marine Sources as a Tool for Functional Food Development. *Front. Mar. Sci.* 9. doi: 10.3389/fmars.2022.832957

He, G. and Ma, R. (2020). Overview of Molecular Mechanisms Involved in Herbal Compounds for Inhibiting Osteoclastogenesis From Macrophage Linage Raw264.7. *Curr. Stem Cell Res. Ther.* 15 (7), 570–578. doi: 10.2174/1574888X14666190703144917

Iglesias, M. J., Soengas, R., Probert, I., Guilloud, E., Gourvil, P., Mehiri, M., et al. (2019). NMR Characterization and Evaluation of Antibacterial and Antiobiofilm Activity of Organic Extracts From Stationary Phase Batch Cultures of Five Marine Microalgae (Dunaliella Sp., D. Salina, Chaetoceros Calcitrans, C. Gracilis and Tisochrysis Lutea). *Phytochemistry* 164, 192–205. doi: 10.1016/j.phytochem.2019.05.001

Jaiswal, K. K., Kumar, V., Vlaskin, M. S. and Nanda, M. (2021). Impact of Pyrene (Polycyclic Aromatic Hydrocarbons) Pollutant on Metabolites and Lipid Induction in Microalgae Chlorella Sorokiniana (UUIND6) to Produce Renewable Biodiesel. *Chemosphere* 285, 131482. doi: 10.1016/j.chemosphere.2021.131482

Jin, W., Yang, L., Yi, Z., Fang, H., Chen, W., Hong, Z., et al. (2020). Anti-Inflammatory Effects of Fucoxanthinol in LPS-Induced RAW264. 7 Cells Through the NAAA-PEA Pathway. *Mar. Drugs* 18 (4), 222. doi: 10.3390/md18040222

Khan, M. I., Shin, J. H. and Kim, J. D. (2018). The Promising Future of Microalgae: Current Status, Challenges, and Optimization of a Sustainable and Renewable Industry for Biofuels, Feed, and Other Products. *Microb. Cell Fact.* 17 (1), 36. doi: 10.1186/s12934-018-0879-x

Krienitz, L., Huss, V. A. and Bock, C. (2015). Chlorella: 125 Years of the Green Survivalist. *Trends Plant Sci.* 20 (2), 67–69. doi: 10.1016/j.tplants.2014.11.005

Kunnumakkara, A. B., Shabnam, B., Girisa, S., Harsha, C., Banik, K., Devi, T. B., et al. (2020). Inflammation, NF-Kappab, and Chronic Diseases: How are They Linked? *Crit. Rev. Immunol.* 40 (1), 1–39. doi: 10.1615/CritRevImmunol.2020033210

Lauritano, C., Andersen, J. H., Hansen, E., Albrigtsen, M., Escalera, L., Esposito, F., et al. (2016). Bioactivity Screening of Microalgae for Antioxidant, Anti-Inflammatory, Anticancer, Anti-Diabetes, and Antibacterial Activities. *Front. Mar. Sci.* 3 (68). doi: 10.3389/fmars.2016.00068

Lin, S. H., Li, M. H., Chuang, K. A., Lin, N. H., Chang, C. H., Wu, H. C., et al. (2020). Chlorella Sorokiniana Extract Prevents Cisplatin-Induced Myelotoxicity *In Vitro* and *In Vivo*. *Oxid. Med. Cell Longev.* 2020, 7353618. doi: 10.1155/2020/7353618

Marangoni, F., Agostoni, C., Borghi, C., Catapano, A. L., Cena, H., Ghiselli, A., et al. (2020). Dietary Linoleic Acid and Human Health: Focus on Cardiovascular and Cardiometabolic Effects. *Atherosclerosis* 292, 90–98. doi: 10.1016/j.atherosclerosis.2019.11.018

Meizlish, M. L., Franklin, R. A., Zhou, X. and Medzhitov, R. (2021). Tissue Homeostasis and Inflammation. *Annu. Rev. Immunol.* 39, 557–581. doi: 10.1146/annurev-immunol-061020-053734

M., U. N., Mehar, J. G.; Mudliar, S. N. and Shekh, A. Y. (2019). Recent Advances in Microalgal Bioactives for Food, Feed, and Healthcare Products: Commercial Potential, Market Space, and Sustainability. *Compr. Rev. Food. Sci. Food Saf.* 18 (6), 1882-1897. doi: 10.1111/1541-4337.12500

Morgese, M. G., Mhillaj, E., Francavilla, M., Bove, M., Morgano, L., Tucci, P., et al. (2016). Chlorella Sorokiniana Extract Improves Short-Term Memory in Rats. *Molecules* 21 (10), 1311. doi: 10.3390/molecules21101311

Niu, S., Yang, L., Zhang, G., Chen, T., Hong, B., Pei, S., et al. (2020). Phenolic Bisabolane and Cuparene Sesquiterpenoids With Anti-Inflammatory Activities From the Deep-Sea-Derived Aspergillus Sydowii MCCC 3A00324 Fungus. *Bioorg. Chem.* 105, 104420. doi: 10.1016/j.bioorg.2020.104420

Obaid, M. L., Camacho, J. P., Brenet, M., Corrales-Orovio, R., Carvajal, F., Martorell, X., et al. (2021). A First in Human Trial Implanting Microalgae Shows Safety of Photosynthetic Therapy for the Effective Treatment of Full Thickness Skin Wounds. *Front. Med. (Lausanne)*. 8. doi: 10.3389/fmed.2021.772324

Olasehinde, T. A., Odjadjare, E. C., Mabinya, L. V., Olaniran, A. O. and Okoh, A. I. (2019). Chlorella Sorokiniana and Chlorella Minutissima Exhibit Antioxidant Potentials, Inhibit Cholinesterases and Modulate Disaggregation of β-Amyloid Fibrils. *Electronic. J. Biotechnol.* 40, 1–9. doi: 10.1016/j.ejbt.2019.03.008

Orecchioni, M., Ghosheh, Y., Pramod, A. B. and Ley, K. (20191084. Macrophage Polarization: Different Gene Signatures in M1(LPS+) vs. Classically and M2(LPS-) vs. Alternatively Activated Macrophages. *Front. Immunol.* 10. doi: 10.3389/fimmu.2019.01084

Pandolfi, F., Franza, L., Carusi, V., Altamura, S., Andriollo, G. and Nucera, E. (2020). Interleukin-6 in Rheumatoid Arthritis. *Int. J. Mol. Sci.* 21 (15), 5238. doi: 10.3390/ijms21155238

Remize, M., Brunel, Y., Silva, J. L., Berthon, J. Y. and Filaire, E. (2021). Microalgae N-3 PUFAs Production and Use in Food and Feed Industries. *Mar. Drugs* 19 (2), 113. doi: 10.3390/md19020113

Riccio, G. and Lauritano, C. (2019). Microalgae With Immunomodulatory Activities. *Mar. Drugs* 18 (1), 2. doi: 10.3390/md18010002

Richmond, A. and Hu, Q. (2013). *Handbook of Microalgal Culture: Applied Phycology and Biotechnology*. 2nd ed. (Hoboken, NJ: Blackwell: John Wiley and Sons).

Rocha, F. G., Brandenburg, M. M., Pawloski, P. L., Soley, B. D. S., Costa, S. C. A., Meinerz, C. C., et al. (2020). Preclinical Study of the Topical Anti-Inflammatory Activity of Cyperus Rotundus L. Extract (Cyperaceae) in Models of Skin Inflammation. *J. Ethnopharmacol.* 254, 112709. doi: 10.1016/j.jep.2020.112709

Senolt, L. (2019). Emerging Therapies in Rheumatoid Arthritis: Focus on Monoclonal Antibodies. *F1000Res* 8. , 1549 doi: 10.12688/f1000research.18688.1

Sibi, G. (2015). Inhibition of Lipase and Inflammatory Mediators by Chlorella Lipid Extracts for Antiacne Treatment. *J. Adv. Pharm. Technol. Res.* 6 (1), 7–12. doi: 10.4103/2231-4040.150364

Tasneem, S., Liu, B., Li, B., Choudhary, M. I. and Wang, W. (2019). Molecular Pharmacology of Inflammation: Medicinal Plants as Anti-Inflammatory Agents. *Pharmacol. Res.* 139, 126–140. doi: 10.1016/j.phrs.2018.11.001

Thiyagarasaiyar, K., Goh, B. H., Jeon, Y. J. and Yow, Y. Y. (2020). Algae Metabolites in Cosmeceutical: An Overview of Current Applications and Challenges. *Mar. Drugs* 18 (6). doi: 10.3390/md18060323

Vieira, M. V., Pastrana, L. M. and Fucinos, P. (2020). Microalgae Encapsulation Systems for Food, Pharmaceutical and Cosmetics Applications. *Mar. Drugs* 18 (12), 644. doi: 10.3390/md18120644

Viola, A., Munari, F., Sanchez-Rodriguez, R., Scolaro, T. and Castegna, A. (2019)1462. The Metabolic Signature of Macrophage Responses. *Front. Immunol.* 10. doi: 10.3389/fimmu.2019.01462

Wen, J., Khan, I., Li, A., Chen, X., Yang, P., Song, P., et al. (2019). Alpha-Linolenic Acid Given as an Anti-Inflammatory Agent in a Mouse Model of Colonic Inflammation. *Food Sci. Nutr.* 7 (12), 3873–3882. doi: 10.1002/fsn3.1225

Yang, L., Li, L., Chen, L., Li, Y., Chen, H., Li, Y., et al. (2015). Potential Analgesic Effects of a Novel N-Acylethanolamine Acid Amidase Inhibitor F96 Through PPAR-Alpha. *Sci. Rep.* 5, 13565. doi: 10.1038/srep13565

Yun, H. S., Kim, Y. S. and Yoon, H. S. (2020). Characterization of Chlorella Sorokiniana and Chlorella Vulgaris Fatty Acid Components Under a Wide Range of Light Intensity and Growth Temperature for Their Use as Biological Resources. *Heliyon* 6 (7), e04447. doi: 10.1016/j.heliyon.2020.e04447

Conflict of Interest: The authors declare that the research was conducted in the absence of any commercial or financial relationships that could be construed as a potential conflict of interest.

Publisher's Note: All claims expressed in this article are solely those of the authors and do not necessarily represent those of their affiliated organizations, or those of the publisher, the editors and the reviewers. Any product that may be evaluated in this article, or claim that may be made by its manufacturer, is not guaranteed or endorsed by the publisher.